

Influence of TiO₂ Particle on the Friction Stir Welding of 7075 Al Alloy



Gautam Behera, Subhadra Sahoo, Nigamananda Ratha, Abhijit Rout, and Manila Mallik

Abstract The effect of TiO₂ particles on the mechanical and corrosion properties of the friction stirred welded 7075 aluminium alloys were studied. Surface topography of the welded samples was carried out with a scanning electron microscope (SEM). Energy dispersive spectroscopy (EDS) was performed to analyze the presence of TiO₂ particles in the weld. The tensile strength of the base 7075 Al alloy was compared with the reinforced and unreinforced weld. The tensile strength of the base alloy is high as compared to weld alloy. The drastic decrease in tensile strength of the welded sample may be ascribed to the dynamic recrystallization followed by grain growth which is the consequence of heat generated due to the friction between the tool and weld material. Residual stresses generated due to welding also affect the strength of the weld. However, the tensile strength of the reinforced alloy is found to be more in contrast to the unreinforced 7075 aluminium alloy. It can be interrelated to the existence of TiO₂ particles which is incorporated in the matrix. The fracture surface was examined through SEM. Overall it shows the ductile mode of fracture. However, in the presence of TiO₂ particle, there is evidence of both intergranular and transgranular fracture. The corrosion behavior was studied by conducting potentiodynamic polarization test with 3.5 wt% NaCl solution. The base alloy shows more corrosion resistance than the unreinforced and reinforced weld.

Keywords Friction stir welding · Stir zone · Nugget · Dimple · Transgranular fracture · Intergranular fracture

1 Introduction

High strength to weight ratio and high fracture toughness of 7075 Al alloy makes it suitable for various applications which include automotive, aerospace, defense, and marine industries [1, 2]. Depending on the area of application, this alloy is joined with the same or different Al alloy. For joining purpose, solid state joining

G. Behera · S. Sahoo · N. Ratha · A. Rout · M. Mallik (✉)
Department of Metallurgical and Materials Engineering, Veer Surendra Sai University of Technology, Burla 768018, Odisha, India

especially solid-state welding has gained a lot of attention. Friction stir welding (FSW) comes under solid state joining which is vastly suggested for Al alloys [3, 4]. It is a hot deformation process where the tool rotates and generates heat by the friction between the tool and the base metal [5]. Welding defects are inevitable, but FSW is confronted with less welding defects. Not only fewer welding defects but the weld portion imparts high mechanical strength also. The joining is possible without the temperature exceeding $0.8 T_m$ (K) and typically, the welding temperature for aluminum 7075 alloy lies between 425 and 480 °C [5]. Many researchers have worked on FSW of 7075 aluminum alloy [4, 5]. In addition to this, some work has also been carried out on friction stir welding of heat treated 7075 alloys to the other grades of aluminium alloy [6]. The change in properties of weld metal is related to the change in microstructure which is associated with structure–property co-relation. Tool geometry, rotating speed of the tool, welding speed, and the prior condition of weld metal are the measure factors that affect the property of the weld metal during FSW. Composite preparation through the addition of reinforcement to the matrix by the process of friction stir welding has gained a lot of attention. Aluminium metal matrix composite has been synthesized successfully by FSW with improved properties and homogeneous distribution of reinforcement. The effect of reinforcement like SiC, TiC, carbon nanotubes (CNT), and TiO₂ has already been studied on different properties of friction stir welding of aluminium alloys [7–12]. Bahrami et al. have studied the effect of SiC on the properties of FSW of 7075 alloy. Both the tensile strength and the toughness are increased due to the amalgamation of SiC nanoparticles in 7075 Al alloy [13]. Lim et al. have used multi-walled carbon nanotube (MWCNT) as a reinforcement in the matrix of Al alloy [12]. It is observed that the factors like the rotation of the tool speed and the penetration of the probe are going to affect the distribution of MWCNT. Homogeneous distribution is achieved when the rotation of the tool is increased from 1500 to 2500 rpm. Micron size SiC particles have also been used as a reinforcement for Al 6351 alloy where the grain growth is restricted due to SiC particles [14]. Mechanical behavior is studied for Al 2618 metal matrix composite reinforced with 20% Al₂O₃ where the tensile test is conducted for the nugget zone at different strain rates and high temperature i.e. in the range of 400–500 °C [15]. Above 10^{-2} s^{-1} strain rate, it shows higher ductility and strain rate sensitivity. Hybrid composite is also synthesized by FSW where SiC and graphite particulate are used as reinforcement in 6063 Al alloy. Surface composite using graphite and graphite + SiC are also synthesized at different volume fractions. SiC particulate reinforced composite shows improved property as compared to graphite and graphite + SiC reinforced composite [8]. Palanivel et al. have worked on the synthesis of Aluminum metal matrix hybrid composite where TiB₂ and BN are used as reinforcement [16]. It is noticed that the wear mode in case of sliding wear is changed from adhesive wear to abrasive wear. As per available literature, no researcher has studied the influence of TiO₂ powder on the mechanical and corrosion properties of FSW of 7075 aluminium alloy.

2 Experimental Procedure

For this study, plates of aluminium 7075 alloy were taken whose dimension was of (12 × 10 × 6) mm³. Welds were produced with and without TiO₂. The average particle size of TiO₂ was in the range of 2–5 μm with a purity of 99%. A groove of 2 mm depth and 1 mm width was prepared along the weld line to accommodate TiO₂ powder in both the plates, which is represented in Fig. 1 (left).

FSW was conducted at a spindle speed of 750 rpm under a load of 100 kg. It was done at a feed rate of 35 mm/min. The FSW was attached with a hot worked tool steel (H13) with a hardness of 52 HRC and the shoulder dia. was 18 mm. The pin dia. and height were 6 and 5.8 mm, respectively. The experimental setup is shown in Fig. 1 (right). The transverse section was polished and etched with Keller's reagent. Then the polished surface was examined with a scanning electron microscope (SU3500 HITACHI SEM). Compositional characterization was done with energy dispersive spectroscopy (Oxford EDS) attached to SEM. The tensile test was done in a universal testing machine (UTE-HGFL-TS-20) and the test sample was prepared according to ASTM E8M-04 standard. The test was done at a rate of 0.003 s⁻¹. The fracture surface of the tensile sample was studied through SEM. The corrosion test was done in POTENTIOSTAT 302 N attached with NOVA 2.1 software. 3.5 wt% NaCl solution was prepared for the test. Platinum and saturated Ag/AgCl were used as counter and reference electrode, respectively. The potential sweep range was from -1 to +1 V. The sample to be corroded was used as a working electrode. The scan rate was 0.05 mV/sec. Optical micrographs of the corroded surface were captured by an optical microscope (Leica DM 1705M).

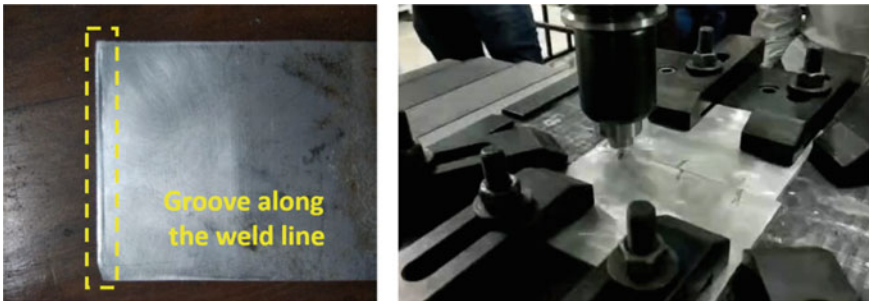


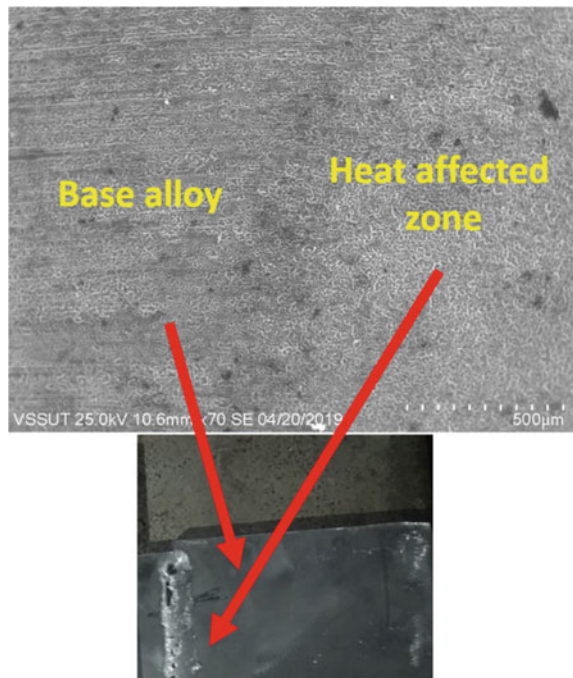
Fig. 1 The groove along the weld line of 7075 aluminium alloy (left) and the tool set up of for FSW of 7075 aluminium alloy (right)

3 Results and Discussion

3.1 Microstructural Characterization

Different zones are created during FSW which comprises of nugget or stir zone (SZ), thermomechanical affected zone (TMAZ), and heat affected zone (HAZ) [17]. Different zones of the unreinforced and reinforced weld are shown in Figs. 2 and 3, respectively. Figure 4 shows the high magnification image of the stir zone with smooth onion rings which symbolize a good weld quality. Onion rings are the characteristic features of the FSW that are formed due to both rotational and translational movement of the probe [18]. In certain cases, onion rings get disappear due to high tool rotational speed, as a result of the easy flowability of the material [19]. Hasan et al. have revealed that there is no deleterious effect of the onion rings on the weld behavior [20]. The distribution of TiO_2 particles is seen in Fig. 5b. It is also verified through EDS (Fig. 5d) where well defined peaks of Ti are present.

Fig. 2 SEM microstructure of base alloy and heat affected zone of FSWed unreinforced 7075 aluminium alloy



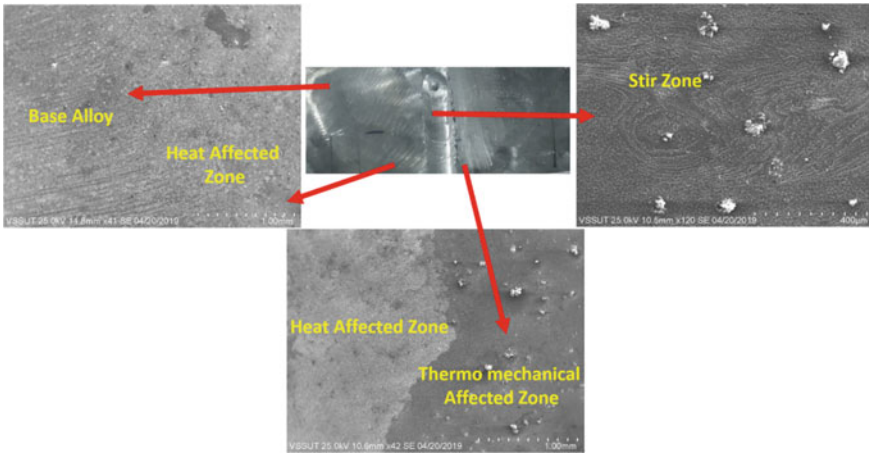


Fig. 3 SEM microstructure of different zones of FSWed 7075 aluminium alloy reinforced with TiO₂ powder

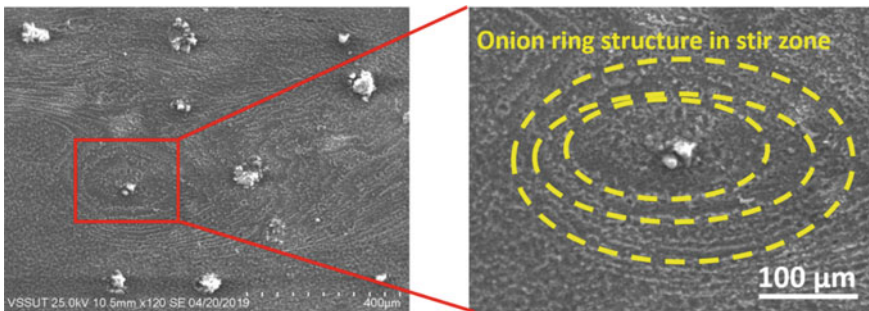


Fig. 4 The presence of onion rings in the SEM image of nugget or stir zone for 7075 aluminium alloy reinforced with TiO₂ powder

3.2 Tensile Test Analysis

The tensile test data is shown in Table 1. This shows that the tensile strength of the base alloy is high as compared to weld alloy. The drastic decrease in tensile strength of the welded sample may be attributed to the dynamic recrystallization followed by grain growth which is the aftermath of heat generated due to the friction between the tool and weld material. Residual stresses generated during welding also affect the strength of the weld. However, the tensile strength of the reinforced alloy is found to be more in contrast to the unreinforced 7075 aluminium alloy. It can be interrelated to the presence of TiO₂ particles in the matrix. Dislocation density is increased due to the thermal mismatch between the reinforced particle and the matrix alloy which in succession increases the strength of the reinforced FSWed sample [21].

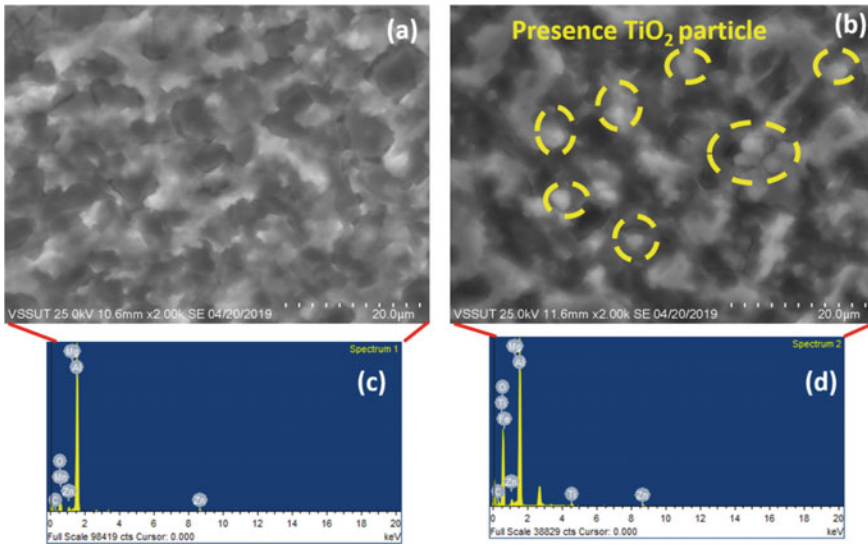


Fig. 5 SEM micrographs of stir zone present in the weld sample: **a** unreinforced and **b** reinforced, and bulk EDS of the weld **c** unreinforced and **d** reinforced

Table 1 Ultimate tensile strength (UTS) of base and FSWed 7075 Al alloy

	Base 7075 Al alloy	FSW without reinforcement	FSW with reinforcement
UTS (MPa)	430.19	132.68	140.42

3.3 Fractography

It is observed from Fig. 6a, b that the mode of fracture is ductile and which is confirmed through the dimple like features present in the SEM micrographs.

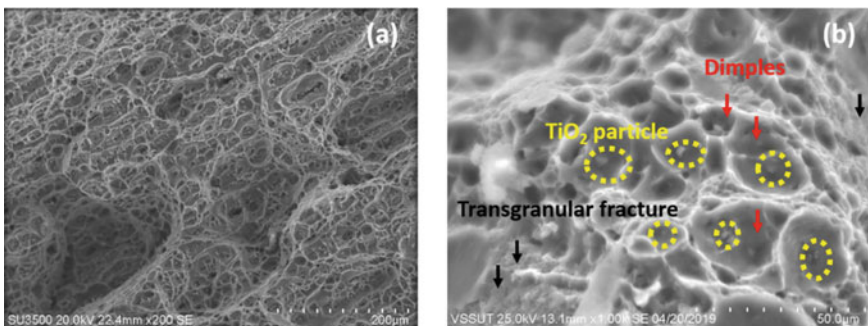


Fig. 6 Fracture surface of the weld 7075 aluminium alloy: **a** unreinforced and **b** reinforced with TiO_2

In the case of a reinforced FSWed sample, TiO₂ particles are partially bulged out from the center of the dimples present in the fractograph. It indicates that the interface between the TiO₂ particle and the matrix acts as the nucleation site for the fracture and the decohesion finally terminates with ductile fracture. Dimples are shown as red arrow marks in Fig. 6b. However, some evidence of transgranular fracture (black arrow mark present in Fig. 6b) is also perceived in some regions of the fracture surface of the reinforced weld.

3.4 Corrosion Plot Analysis

It is observed from the corrosion plot (Fig. 7) and Table 2 that the base 7075 Al alloy shows higher corrosion resistance than the reinforced as well as unreinforced weld. The diminution of corrosion resistance in the weld is due to the welding defect and residual stress generated during welding. It has already been revealed that 7075 alloy is a precipitation strengthened alloy. The precipitate gets coarsen as the

Fig. 7 The potentiodynamic polarization curve for base alloy, unreinforced and reinforced weld, and HAZ of reinforced weld

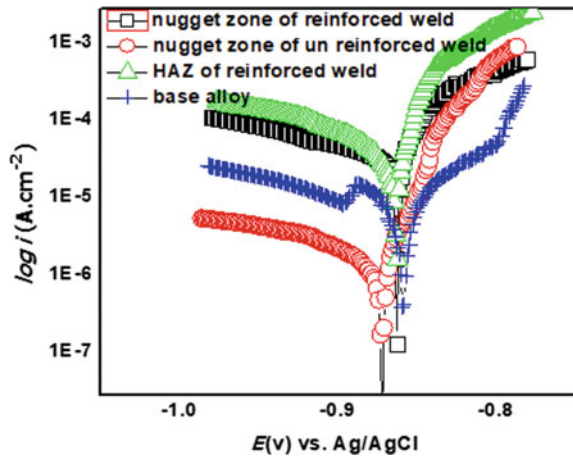


Table 2 The parameters for potentiodynamic curves

Different regions of sample	I_{corr} (mA/cm ²)	$-E_{corr}$ (mV vs. SCE)
Unreinforced weld (Stir zone)	1.077E-02	862.97
Reinforced weld (Stir zone)	4.302E-04	871.24
Reinforced weld (HAZ)	4.0304E-02	848.3
Base alloy	3.7005E-04	858.26

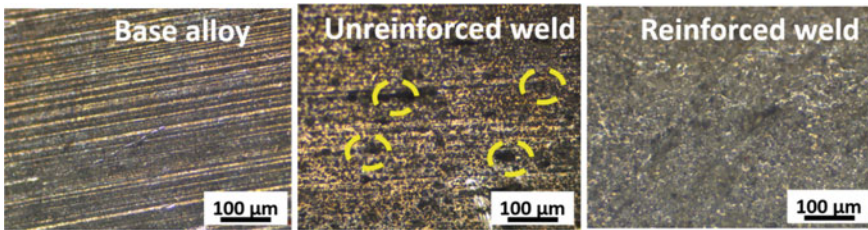


Fig. 8 Optical micrographs of pits formed due to corrosion in base alloy, unreinforced and reinforced weld

welding temperature reaches the mushy state temperature. A galvanic cell is developed between the precipitate and the matrix where the precipitates formed in grain boundary acts as a cathode and the rest area behaves as an anode [22]. However, the corrosion is a pitting type of corrosion which is visible in Fig. 8. The pitting corrosion mainly depends on the chloride ion concentration [23]. The improvement in corrosion resistance of reinforced weld is because of the passivation provided by uniformly distributed TiO_2 particles in an aluminium alloy matrix. Uniform distribution of TiO_2 particles also prevents the formation of a galvanic cell.

4 Conclusions

- i. Reinforced particle i.e., TiO_2 was successfully incorporated into 7075 aluminium alloy through friction stir welding. These are uniformly distributed in the matrix.
- ii. The tensile strength of TiO_2 reinforced weld is more than the unreinforced weld sample. The reduction in tensile strength of the weld sample in comparison to the base alloy sample is due to dynamic recrystallization followed by grain growth. The increase in tensile strength of the reinforced weld is due to the addition of TiO_2 particles.
- iii. Ductile fracture is observed in both unreinforced and reinforced TiO_2 weld. There was some sign of transgranular type brittle fracture in the reinforced weld.
- iv. The base alloy shows higher corrosion resistance than the weld. The incorporation of the reinforced particle increases the corrosion resistance of the weld alloy. Pitting type of corrosion is observed in weld alloy and the improvement in corrosion resistance of reinforced weld is because of the passivation provided by uniformly distributed TiO_2 particles in an aluminium alloy matrix.

References

1. Su JQ, Nelson TW, Mishra R, Mahoney M (2003) Microstructural investigation of friction stir welded 7050–T651 aluminium. *Acta Mater* 51(3):713–729
2. Shen Z, Yang X, Zhang Z, Cui L, Li T (2013) Microstructure and failure mechanisms of refill friction stir spot welded 7075–T6 aluminum alloy joints. *Mater Des* 44:476–486
3. Gerlich A, Avramovic-Cingara G, North TH (2006) Stir zone microstructure and strain rate during Al 7075-T6 friction stir spot welding. *Metall Mater Trans A* 37(A):2773–2786
4. Israr JJP, Israr M (2017) Experimental investigation of friction stir welding of aluminium alloy AA7075 for various process parameters. *Int J Mech Solids* 12(2):169–177
5. Kumar PV, Reddy GM, Rao KS (2015) Microstructure, mechanical and corrosion behavior of high strength AA7075 aluminium alloy friction stir welds—effect of post weld heat treatment. *Def Technol* 11(4):362–369
6. Kumar SK, Kumar P (2016) Study the effect of parameters of friction stir welding on the impact strength of aluminium 6063. *Int J Curr Eng Technol* 6(3):993–998
7. Tabasi M, Farahani M, Besharati Givi MK, Farzami M, Moharami A (2015) Dissimilar friction stir welding of 7075 aluminum alloy to AZ31 magnesium alloy using SiC nanoparticles. *Int J Adv Manuf Technol*
8. Dhayalan R, Kalaiselvan K, Sathiskumar R (2014) Characterization of AA6063/SiC-Gr surface composites produced by FSP technique. *Procedia Eng* 97:625–631
9. Bahrami M, Helmi N, Dehghani K, Kazem M, Givic B (2014) Exploring the effects of SiC reinforcement incorporation on mechanical properties of friction stir welded 7075 aluminum alloy: fatigue life, impact energy, tensile strength. *Mater Sci Eng A* 595:173–178
10. Uzun H (2007) Friction stir welding of SiC particulate reinforced AA2124 aluminium alloy matrix composite. *Mater Des* 28:1440–1446
11. Mirjavadi SS, Alipour M, Emamian S, Kord S, Hamouda AMS, Koppad PG, Keshavamurthy R (2017) Influence of TiO₂ nanoparticles incorporation to friction stir welded 5083 aluminum alloy on the microstructure, mechanical properties and wear resistance. *J Alloy Compd* 712:795–803
12. Lim DK, Shibayanagi T, Gerlich AP (2009) Synthesis of multi-walled CNT reinforced aluminium alloy composite via friction stir processing. *Mater Sci Eng A* 507(1):194–199
13. Bahrami M, Helmi N, Dehghani K, Givi MKB (2014) Exploring the effects of SiC reinforcement incorporation on mechanical properties of friction stir welded 7075 aluminum alloy: Fatigue life, impact energy, tensile strength. *Mater Sci Eng A* 595:173–178
14. Karthikeyan P, Mahadevan K (2015) Investigation on the effects of SiC particle addition in the weld zone during friction stir welding of Al 6351 alloy. *Int J Adv Manuf Technol* 80(9):1919–1926
15. Cavaliere P (2005) Mechanical properties of friction stir processed 2618/Al₂O₃/20p metal matrix composite. *Compos A Appl Sci Manuf* 36(12):1657–1665
16. Palanivel R, Dinaharan I, Laubscher RF, Davim JP (2016) Influence of boron nitride nanoparticles on microstructure and wear behavior of AA6082/TiB₂ hybrid aluminum composites synthesized by friction stir processing. *Mater Des* 106:195–204
17. Thota V, Rao K, Kalvala P (2004) Studies on friction stir welded AA 7075 aluminum alloy. *Trans Indian Inst Met* 57:659–663
18. Krishnan KN (2002) On the formation of onion rings in friction stir welds. *Mater Sci Eng A* 327(2):246–251
19. Weng F, Liu Y, Chew Y, Lee BY, Ng FL, Bi G (2020) Double-side friction stir welding of thick magnesium alloy: microstructure and mechanical properties. *Sci Technol Weld Joining* 25(5):359–368
20. Hasan MM, Ishak M, Rejab MRM (2017) Effect of pin tool design on the material flow of dissimilar {AA}7075-{AA}6061 friction stir welds. *IOP Conf Ser Mater Sci Eng* 257:12022
21. Akbari MK, Baharvandi HR, Shirvanimoghaddam K (2015) Tensile and fracture behavior of nano/micro TiB₂ particle reinforced casting A356 aluminum alloy composites. *Mater Des* 1980–2015(66):150–161

22. Gharavi F, Matori K, Yunus R, Othman NK, Fadaeifard F (2015) Corrosion behavior of Al6061 alloy weldment produced by friction stir welding process. *J Mater Res Technol* 31
23. Corral J, Trillo E, Li Y, Murr L (2000) Corrosion of friction-stir welded aluminum alloys 2024 and 2195. *J Mater Sci Lett* 19:2117–2122